

Development of Fatigue Testing System for in-situ Observation by AFM & SEM

Amir Farokh Payam^{1,2}, Oliver Payton³, Mahmoud Mostafavi¹, Loren Picco⁴, Stacy Moore³, Tomas Martin³, A.D. Warren³, David Knowles¹

¹Solid Mechanics Research Group, Department of Engineering, University of Bristol, Bristol, UK

²School of Engineering, Ulster University, Belfast, UK.

³Interface Analysis Centre, HH Wills Physics Laboratory, University of Bristol, Bristol, UK

⁴Department of Physics, Virginia Commonwealth University, Virginia, USA

Abstract. A three-point bend fatigue miniature stage for in-situ observation of fatigue microcrack initiation and growth behaviour by scanning electron microscopy (SEM) and atomic force microscopy (AFM) has been manufactured. Details of the stage design with finite element analysis of the stress profiles on loading are provided. The proposed stage facilitates study of the micro mechanisms of fatigue when used during SEM and AFM scanning of the sample surface. To demonstrate the applicability of the system, fatigue tests have been performed on annealed AISI Type 316 stainless steel. Surface topography images obtained by SEM and HS-AFM (High Speed AFM) are presented for comparison. The data can be used to validate crystal plasticity models which should then directly predict multiaxial behaviour without recourse to deformation rules such as equivalent stress or strain.

1 Introduction

Fatigue damage evolution in macroscopically defect-free metallic systems requires local cyclic plasticity as a result of the application of repeated stress; ultimately this leads to crack initiation [1] and growth. Three principal steps which may be observed in the fatigue process of engineering structures are: initiation, including nucleation and micro growth, crack growth and ultimate failure [2]. Intragranular slip band formation evident on the free polished surface of a stressed specimen is the first sign of fatigue damage which can lead to crack initiation in many metallic systems [3]. While numerous theoretical and computational techniques have been developed to investigate fatigue crack initiation and growth such as [4]–[14], physical evidence and high resolution validation data for fatigue nucleation, initiation and growth relies upon the development of experimental methods and observations. Recent modelling advancement such as crystal plasticity and dislocation dynamics approaches have provided the opportunity to model mesoscale plasticity in considerable detail. However, because of the complexity of the local strain fields, high resolution study at the grain and sub-grain level is required to validate and interrogate these models rigorously. In this paper, the design of a three-point test miniature stage which is compatible with AFM sample holder requirements is presented, in the context of in-situ micro fatigue damage monitoring using SEM and AFM. As a result of loading on the

The stage, with integral loading points, was manufactured from EN24 steel by wire electro discharge machining. Image of the finished stage and how it fits into the loading machine is given in Fig.2. The loading machine used in our experiment was an Instron 1341 with a 1 kN load cell that is driven hydraulically. Cyclic deformation tests were performed with 250 MPa peak surface stress (1000 and 10000 cycles) in a three-point flexure bend approach. The sinusoidal load with a frequency of 2 Hz was applied to the beam. After termination of loading process, the sample was locked and maintained under load. Then the stage could be moved to the SEM/HS-AFM for imaging and characterization, supported through the loading pin onto the stage.

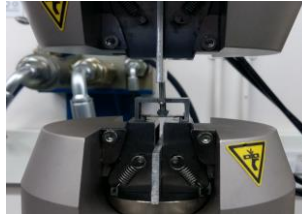


Fig. 2. Photos showing the rig under Load.

2.3 HS-AFM Measurement

HS-AFM affords a major benefit over conventional AFM when considering fatigue as it is possible to rapidly image the deformed surface of the material with sub nanometre height resolution and nanometre lateral resolution, generating multiple megapixel frames per second. In this study a contact mode HS-AFM (Bristol Nano Dynamics Ltd, UK) was employed [17], [18] to gather data on the samples. Critically, the architecture of the system enabled enough height clearance for the micro-strain rig to be mounted in the microscope. Although the sample scanning nature of the tool dictates that the rig be light weight so as not to degrade the motions of the scanner.

The large area imaging mode of the HS-AFM allowed areas 100s μm in length to be explored in under an hour with no deterioration in lateral resolution. As HS-AFM, like all AFMs, measures the sample topography, it is possible to measure the true height of the slip bands on the surface with sub-atomic resolution (± 15 pm), which is less than the central spacing between closed pack atoms (analogous to one Burgers vector).

3 Results and Discussion

Fig. 3 illustrates secondary electron SEM images of the pre/post loaded annealed stainless steel beam (10000 cycles) with a maximum stress of ~ 250 MPa at the centre of the beam; the 0.2% proof stress of the material is 290 MPa. As can be seen from Fig.3-b, at the centre of the sample, slip bands appeared in the grains. Clearly the deformation at the centre of the specimen, although slightly below the large scale proof stress, produces larger strains which cause more slip bands in the centre region. When the sample is loaded, slip lines, related to local plastic deformation are evident as traces across the individual grains. Increasing the load clearly leads to the increase of the density and height of such slip lines. Fig. 3-b shows that at the centre of the specimen some grains have fully developed sets of slip bands, while the neighbouring grains have little surface deformation. This can be explained by the fact that the formation and development of slip bands at the grains strongly depends on the orientation of slip active system inside the grains relative to the applied major principal stress, somewhat modified by the neighbouring grain environment. So, based on the

orientation of active slip systems towards the surface of material and the orientation of the trace of slip systems with loading axis, the formation and growth of slip bands at the grains are different.

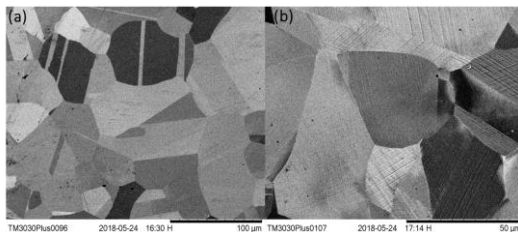


Fig. 3. Pre-loading SEM (a), post-loading SEM of the centre (b).

To analyse the slip height and separation of the slip bands in each grain, we studied individual HS-AFM frames from our measurements. In this preliminary study, three factors of fatigue damage evolution: i) the slip height, ii) the separation distance between slips, and iii) the number of slip bands are considered.

The quantitative results of the measured grains at the $39 \times 35 \mu\text{m}^2$ area of the centre of sample are presented in Figs.4-5. For the limited number of grains studied the probability distribution function map of slip heights and separation distances after 1000 cycles are shown in Fig.4-a. As can be seen, the majority of slip band spacings are around 2.5 - 3 μm and the majority of slip heights are around 1.5 - 2 nm. The maximum observed slip height is 8.5 nm and minimum observable slip height is around 0.25 nm which is comparable with one Burgers vector translation. Recognising that the angle which the Burgers vector subtends relative to the surface plane normal has not been presented here. Figs. 4-b shows a frame of HS-AFM measurements. Above a certain stress applied to the sample, more slip bands are activated in some grains due to the loading orientation. This can be explained by the local stresses being high enough to release a new and more closely spaced slip bands [19].

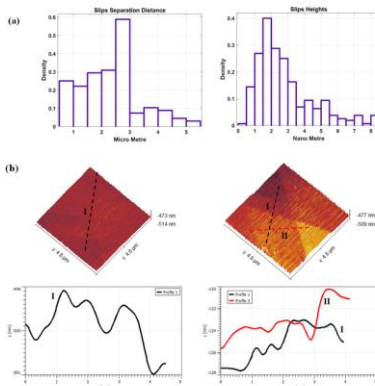


Fig. 4. Shows a) probability distribution map of slips separation distance and height after 1000 cycles. HS-AFM topographic maps of the surface inside two different grains after 1000 cycles. The arrows indicate the trace of the slip planes: b) different orientations. The profiles I, II taken along the lines I and II respectively show steps. The lines are started from left to right.

Fig.5 shows the quantitative results of the measured grains for loading after 10000 cycles. The probability distribution function map of slip heights and separation distances are shown in Fig.5-a. The single frame HS-AFM topography maps of a surface inside the measured grains after 10000 cycles loading are shown in Fig 5-b. Because of strain accumulation after 10000 cycles loading, there is an increase in the number of slip bands which clearly

appear in the quantitative results. The maximum slip height is 43 nm and the minimum one is 0.25 nm. The minimum slip height is comparable with one Burgers vector translation. In comparison with 1000 cycles loading, the average slip separation distance for the 10000 cycles loading is decreased which is expected from the initiation and formation new slip bands between the existent slip bands produced in previous cycles. This means that during cyclic loading, which leads to the fatigue crack initiation, both the creation of new slip bands and an increase in irreversible plastic strain has occurred. This is illustrated by the results shown in Fig.5-b which consists of different slip heights.

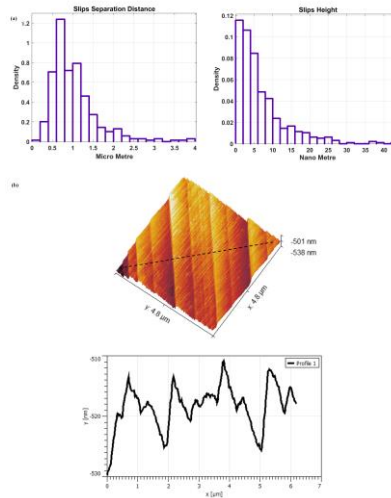


Fig. 5. shows a) probability distribution map of slips separation distance and height after 10000 cycles. HS-AFM topographic maps of the surface inside different measured grains after 10000 cycles as an illustrative example which have been used to generate data in (a). The arrows indicate the trace of the slip planes: b) one orientations. The profile taken along the line show steps. The lines are started from left to right.

From the quantitative analysis of our measurement results, it can be summarized that the larger slip heights are corresponded to the slip bands which are initiated at the first cycles and grow by strain accumulation in subsequent cycles. The smaller slip height regions are related to the new initiated slips due to strain accumulation in higher cycles loading, for which there is an element of an initiation period. Here, due to the initiation and formation of new slips, the distribution and average of slip separation are decreased, which means the presence of more slips and formation of slip parallel to the previous slip bands. It is important to mention that the development of slip bands inside the grains is strongly dependant on the orientation of the active slip systems, which will be considered in our future study. In the current study, our first aim is to validate the performance of our designed miniature stage and show the capability of HS-AFM to provide topographic maps of large scan areas of the surface of specimen which consist of different grains. The second aim of our current study is to show the ability of HS-AFM to provide quantitative analysis of measured grains focusing on the number of slip bands, distribution and formation of slip heights and distances at different cycles of loading. To improve the comprehensiveness of quantification and analysis, the subsequent step will be the determination of the specific grain's orientation measured by EBSD and focus the HS-AFM measurements on the interested regions cycle by cycle. In this manner, based on the proposed methodology, the evolution of slip bands and initiation of fatigue in each cycle can be analysed, and the effect of grain orientations on the fatigue initiation/growth can be explored. These data can be

used to validate crystal plasticity models which should then directly predict multiaxial behaviour without recourse to deformation rules such as equivalent stress or strain.

4 Conclusion

In this paper, the design process of a miniature three-point bending fatigue testing stage for in-situ observation of microcrack initiation and growth behaviour by SEM and contact mode HS-AFM is presented. Using FEA the loading mechanism of the proposed stage is simulated and the stress concentration on the surface of the specimen is analysed. Then, to study in-situ the fatigue behaviour of annealed AISI type 316 stainless steel, the manufactured stage is used. There is a good agreement between SEM results of the surface before and after the loading with finite element simulations. Then, HS-AFM is used to provide the three-dimensional images of the surface and quantify the height and space of slip-bands at different grains. The HS-AFM results clearly shows different height and space of slip bands at different grains based on the cycling and plane orientations. The results are a proof of principle aimed at calibrating CP models which can then be tested under biaxial conditions with a future focus on damage evolution.

References

1. J. Schijve, *Fatigue of Structures and Materials*. Springer, Dordrecht, (2009).
2. P. P. Milella. *Fatigue and Corrosion in Metals*. Springer-Nature, (2013).
3. J.-Y. Buffiere. Fatigue Crack Initiation And Propagation From Defects In Metals: Is 3D Characterization Important?. *Procedia Struct Integr*, **7**: 27–32 (2017).
4. C. F. R. & M. C. F. C. Déprés. Low-strain fatigue in 316L steel surface grains: a three dimension discrete dislocation dynamics modelling of the early cycles. Part 2: Persistent slip markings and micro-crack nucleation title. *Philos Mag*, **86** (1): 79–97 (2006).
5. N. Merah, F. Saghir, Z. Khan, and A. Bazoune. A study of frequency and temperature effects on fatigue crack growth resistance of CPVC. *Eng Fract Mech*, **72**(11):1691–1701 (2005).
6. Z. S. Hosseini, M. Dadfarnia, B. P. Somerday, P. Sofronis, R. O. Ritchie. On the theoretical modeling of fatigue crack growth. *J Mech Phys Solids*, **121**: 341–362 (2018).
7. Z. Zhang, D. Lunt, H. Abdolvand, A. J. Wilkinson, M. Preuss, F. P. E. Dunne. Quantitative investigation of micro slip and localization in polycrystalline materials under uniaxial tension. *Int J Plast*, **108**: 88–106 (2018).
8. Z. Zheng, A. Stapleton, K. Fox, F. P. E. Dunne. Understanding thermal alleviation in cold dwell fatigue in titanium alloys. *Int J Plast*, (2018).
9. A. Guery, F. Hild, F. Latourte, S. Roux. Slip activities in polycrystals determined by coupling DIC measurements with crystal plasticity calculations. *Int J Plast*, **81**: 249–266 (2016).
10. A. Ueno H. Kishimoto. Development of in situ observation fatigue testing systems and their application, in *Fatigue*. In: *Proceedings of the Seventh International Fatigue Congress*, Vol. 4/4.
11. J. Y. Huang, J. J. Yeh, S. L. Jeng, C. Y. Chen, R. C. Kuo. High-cycle fatigue behavior of type 316L stainless steel. *Mater Trans*, **47**(2): 409–417 (2006).

12. A. J. Wilkinson T. Ben Britton. Strains, planes, and EBSD in materials science. *Mater Today*,15(9): 366–376 (2012).
13. A. Barrios, S. Gupta, G. M. Castelluccio, O. N. Pierron. Quantitative in Situ SEM High Cycle Fatigue: The Critical Role of Oxygen on Nanoscale-Void-Controlled Nucleation and Propagation of Small Cracks in Ni Microbeams. *Nano Lett*, 18(4): 2595–2602 (2018).
14. G. Biallas, H. J. Maier. In-situ fatigue in an environmental scanning electron microscope - Potential and current limitations. *Int J Fatigue*, 29(8): 1413–1425 (2007).
15. Sandmeyer Steel Specification Sheet: Alloy 316/316L. 1: 3 (2014).
16. A. D. Warren, A. I. Martinez-Ubeda, O. D. Payton, L. Picco, T. B. Scott. Preparation of Stainless Steel Surfaces for Scanning Probe Microscopy. *Micros Today*, 24(3): 52–55 (2016).
17. A. Laferrere, R. Burrows, C. Glover, R. N. Clark, O. Payton, L. Picco, S. Moore, G. Williams. In situ imaging of corrosion processes in nuclear fuel cladding. *Corros Eng Sci Technol*, 52(8): 596–604 (2017).
18. S. Moore, R. Burrows, L. Picco, T. Martin, S. Greenwell, T. Scott, O. Payton. A study of dynamic nanoscale corrosion initiation events by HS-AFM. *Faraday Discuss*, (2018).
19. F. A. Martin, J. Cousty, C. Bataillon. In situ AFM study of pitting corrosion and corrosion under strain on a 304L stainless steel. *Congr Proc EUROCORR*, 16(12): 1–10 (2004).